

## Probing for primary functions of prohibitin in *Trypanosoma brucei*

Jiří Týč<sup>a</sup>, Drahomíra Faktorová<sup>a</sup>, Eva Kriegová<sup>a</sup>, Milan Jirků<sup>a</sup>, Zuzana Vávrová<sup>a</sup>, Dmitri A. Maslov<sup>b,\*</sup>, Julius Lukeš<sup>a,\*</sup>

<sup>a</sup> Biology Centre, Institute of Parasitology, Czech Academy of Sciences, and Faculty of Natural Sciences, University of South Bohemia, České Budějovice (Budweis), Czech Republic

<sup>b</sup> Department of Biology, University of California, Riverside, CA 92521, USA

### ARTICLE INFO

#### Article history:

Received 12 March 2009  
Received in revised form 9 July 2009  
Accepted 10 July 2009

#### Keywords:

Prohibitin  
*Trypanosoma*  
Mitochondrion  
Morphology  
Mitochondrial translation

### ABSTRACT

Prohibitins (PHBs) 1 and 2 are small conserved proteins implicated in a number of functions in the mitochondrion, as well as in the nucleus of eukaryotic cells. The current understanding of PHB functions comes from studies of model organisms such as yeast, worm and mouse, but considerable debate remains with regard to the primary functions of these ubiquitous proteins. We exploit the tractable reverse genetics of *Trypanosoma brucei*, the causative agent of African sleeping sickness, in order to specifically analyse the function of PHB in this highly divergent eukaryote. Using inducible RNA interference (RNAi) we show that PHB1 is essential in *T. brucei*, where it is confined to the cell's single mitochondrion forming a high molecular weight complex. PHB1 and PHB2 appear to be indispensable for mitochondrial translation. Their ablation leads to a decrease in mitochondrial membrane potential, however no effect on the level of reactive oxygen species was observed. Flagellates lacking either PHB1 or both PHB1 and PHB2 exhibit significant morphological changes of their organelle, most notably its inflation. Even long after the loss of the PHB proteins, mtDNA was unaltered and mitochondrial cristae remained present, albeit displaced to the periphery of the mitochondrion, which is in contrast to other eukaryotes.

© 2009 Australian Society for Parasitology Inc. Published by Elsevier Ltd. All rights reserved.

### 1. Introduction

Prohibitins (PHBs) comprise evolutionary conserved proteins ubiquitously present in eukaryotes, where they were proposed to function in multiple capacities. They consist primarily of PHB1 and a closely related PHB2, sometimes called prohibitone. As suggested by the name, PHBs were originally associated with regulation of cell-cycle proliferation (McClung et al., 1989), although this function was later challenged (Manjeshwar et al., 2003). Since the time of their original description, PHBs have been localised to several cellular compartments such as the mitochondrion, nucleus and cell membrane, and have been implicated in an ever increasing number of cellular processes, such as apoptosis, transcriptional control, cell signalling, senescence and mitochondrial biogenesis (for recent reviews see Mishra et al., 2005; Merkwirth and Langer, 2009).

In mitochondria of *Saccharomyces cerevisiae*, *Caenorhabditis elegans* and humans, the PHB proteins are assembled into a large ring-like inner membrane protein complex, the existence of which is supported by mutual dependence of PHB1 and PHB2 (Tatsuta

et al., 2005). Both proteins co-immunoprecipitate (Coates et al., 2001) and the elimination of one PHB leads to the disappearance of the other (Berger and Yaffe, 1998; Artal-Sanz et al., 2003; Merkwirth et al., 2008). The PHB complex was proposed to be critical for proper folding and stabilization of mitochondrial-encoded subunits of respiratory complexes (Nijtmans et al., 2000; Bourges et al., 2004) and its depletion is followed by apoptosis and fragmentation of mitochondria (Kasashima et al., 2006).

However, growing evidence from several organisms favours the association of PHB function primarily with mitochondrial morphology, corroborating the early observations from *C. elegans* (Artal-Sanz et al., 2003). The PHB proteins appear to be critical for organellar integrity (Sun et al., 2008), in particular in the morphogenesis of mitochondrial cristae and for the proper function of another mitochondrial protein, OPA1, with which they interact (Merkwirth et al., 2008). Putative interactions of PHBs with the inner membrane  $F_1F_0$ -ATP synthase-specific chaperones (Osman et al., 2007) can be interpreted as a potential scaffolding function of the PHB complex (Merkwirth and Langer, 2009). Furthermore, in human mitochondria, PHB1 was recently implicated in the maintenance of mtDNA within the mitochondrial nucleoids, as well as in regulation of its copy number within the organelle (Kasashima et al., 2008).

A more extensive list of putative functions is associated with the extramitochondrial PHBs. Their anti-proliferative function,

\* Corresponding authors. Address: Biology Centre, Branišovská 31, 37005 České Budějovice, Czech Republic. Tel.: +420 38 7775416; fax: +420 38 5310388.

E-mail addresses: [maslov@ucr.edu](mailto:maslov@ucr.edu) (D.A. Maslov), [jula@paru.cas.cz](mailto:jula@paru.cas.cz) (J. Lukeš).

corroborated by the analysis of a conditional mouse mutant (Merkwirth et al., 2008), could be due to their interaction with the retinoblastoma and p53 proteins (Fusaro et al., 2003). However, circumstantial evidence indicates that other processes might explain the anti-proliferative and anti-apoptotic effects of PHBs (Mishra et al., 2005). Their expression decreases in response to oxidative stress, and they are down-regulated in human Crohn's disease and colitis (Theiss et al., 2007). As a reflection of their significant homology with the oestrogen receptor co-repressor, PHBs can repress androgen receptor-mediated transcription and thus androgen-dependent growth of prostate cells (Gamble et al., 2007). The PHB proteins are strongly up-regulated upon activation of primary human T cells (Ross et al., 2008). Since PHB1 is up-regulated in chronic schizophrenia, it has been speculated that it might be causally involved in the disease process (Smalla et al., 2008). Furthermore, PHB1 has been found to be over-expressed in various cancer cells, and since this protein induces a block at the G0/G1 phase of the cell cycle, it promotes their survival (Gregory-Bass et al., 2008). Thus, silencing of PHB1 might prove to be a promising therapeutic approach against certain forms of cancer. The prominence of PHBs in various cancer cells, their binding to tumour-suppressor proteins and their anti-estrogen action qualify PHBs as promising new targets for cancer therapy (Mishra et al., 2005). Similarly, their unique chaperonine function in the mitochondrion implicates PHBs in complex phenotypes such as longevity, obesity and anti-oxidant defence. Since PHBs have to date resisted all attempts at crystallization, our knowledge of their structure is derived solely from predictions.

One of the reasons for our fragmented knowledge about these apparently multi-functional and highly important proteins is the difficulty associated with disentangling various functions of PHBs in complex multicellular organisms. It was shown that the yeast null mutant for PHB1 has a decreased lifespan accompanied by a decrease in mitochondrial membrane potential (Coates et al., 1997), whilst it becomes lethal in combination with mutations in either the mitochondrial inheritance machinery (Berger and Yaffe, 1998), the AAA-proteases (Steglich et al., 1999) or the phosphatidylethanolamine biosynthetic process (Birner et al., 2003). Whilst inactivating the gene in *Drosophila melanogaster*, *C. elegans* and mammals demonstrated its essentiality for development of these organisms (Artal-Sanz et al., 2003; Park et al., 2005), the primary reason for the lethal phenotype remains elusive. Tissue-specific conditional disruption of PHB2 in mouse is a very powerful approach (Merkwirth et al., 2008), yet it also faces the difficulty of determining which phenotypic effects are primary and which are only secondary.

*Trypanosoma brucei* is a parasitic protist responsible for lethal African sleeping sickness of humans. This flagellate, together with the related kinetoplastids such as *Trypanosoma cruzi* and *Leishmania* spp., is responsible for millions of disease cases worldwide. Separation of the kinetoplastid phylogenetic lineage from most other eukaryotes occurred very early in evolution (Brinkmann and Philippe, 2007). Therefore, by analysing the function of PHBs in this highly divergent system, it might be possible to reveal the primary functions of PHBs that have been universally preserved in all eukaryotes. In the present report, we have shown that in trypanosomes PHB1 is confined to the mitochondrion and is critical for organellar translation and morphology. All detected phenotypic consequences of its down-regulation by RNA interference (RNAi) appear to be mitochondrion-derived. These functions can be considered the primary functions, whilst the wide range of other functions strongly or weakly associated with PHB in multicellular systems have likely been acquired later in eukaryotic evolution.

## 2. Materials and methods

### 2.1. Phylogenetic analysis

The PHB1 and PHB2 homologues have been annotated in the gene database that includes the sequenced genomes of *T. brucei*, *T. cruzi*, *Leishmania major*, *Leishmania braziliensis* and *Leishmania infantum* ([www.genedb.org](http://www.genedb.org)). The following PHB sequences have been selected from the non-redundant protein sequences database by a high score in the NCBI protein Blast search using as queries the trypanosomatid PHB1 and PHB2 sequences, respectively:

Metazoa: *Acyrtosiphon pisum* (NP\_001119688 and XP\_001952808), *Branchiostoma floridae* (EEA76736 and EEA56573), *Culex quinquefasciatus* (XP\_001848602 and XP\_001842651), *D. melanogaster* (NP\_724165 and NP\_001097372), *Homo sapiens* (AAS88903 and NP\_009204), *Salmo salar* (NP\_001133602 and NP\_001134876), *Xenopus laevis* (NP\_001079486 and NP\_001086635); fungi: *Coprinopsis cinerea* (XP\_001828913 and XP\_001835707), *Malassezia globosa* (XP\_001730789 and XP\_001730682), *Neurospora crassa* (CAD71006 and XP\_964487), *S. cerevisiae* (EDN61723 and EDN61816); plants: *Arabidopsis thaliana* (AAM64845 and NP\_171882), *Chlamydomonas reinhardtii* (XP\_001696940 and XP\_001701753), *Oryza sativa* (EAY86430 and NP\_001051853), *Zea mays* (ACG34005 and ACG33462), *Physcomitrella patens* (XP\_001756758 and XP\_001760222); stramenopiles (diatoms): *Phaeodactylum tricorutum* (EEC45057 and EEC48099); Apicomplexa: *Plasmodium falciparum* (XP\_001349234 and XP\_001347429), *Theileria parva* (XP\_763427 and XP\_765715), *Toxoplasma gondii* (EEA99743 and EEB01029); and Amoebozoa: *Dictyostelium discoideum* (XP\_635884 and XP\_638766). The sequences were aligned using Clustal X 2.0.10 (Larkin et al., 2007). The poorly aligned N- and C-termini and alignment gaps were removed. The final alignment was 207 residues long. The minimal evolution analysis was performed by MEGA 4.0.2 (Tamura et al., 2007) using the Dayhoff PAM matrix of amino acid substitution and  $\gamma$ -distribution of variable sites with bootstrap (1,000 replicates).

### 2.2. Generation of RNAi-knock-down cell lines

Vectors pLew100 and p2T7-177 with single and opposing T7 promoters, respectively, were used for the preparation of RNAi knock-down cell lines in the *T. brucei* procyclic form. A 525 nucleotide (nt) long 5' region of the PHB1 gene was amplified using primers Ph1-F1 (5'-AAGCTTGGATCCAGCGTTTATGCTTGGAG-3') (added XbaI and BamHI restriction sites are underlined) and Ph1-R1 (5'-TCTAGAGGATCCTTACCGAACTGAATATCCAC-3') (added HindIII and BamHI restriction sites are underlined) from genomic DNA of the *T. brucei* strain 29-13. The amplified fragment was first digested with the BamHI restriction enzyme and cloned into the BamHI-linearised pLew100 vector. Plasmid with the PHB1 gene oriented in the downstream direction with respect to the single T7 promoter was selected by restriction analysis and named pLew100-PhA. Next, the above-described PCR amplicon was digested with the XbaI and HindIII restriction enzymes and cloned into the pLew100-PhA construct linearised with the appropriate enzyme, so that the second version of the PHB1 gene was in the opposite direction with respect to the first PHB1 gene.

Another cell line, in which the PHB1 gene can be down-regulated by RNAi, was prepared by cloning a fragment of the PHB1 gene amplified with the primers Ph1-F1 and Ph1-R1, and digested with restriction enzymes BamHI and HindIII into the p2T7-177 vector, creating the p2T7-PhB construct. Finally, a double knock-down for the PHB1 and PHB2 genes (PHB1 + 2) was prepared as follows. The 5' part of the PHB2 gene spanning nts 1–410 was amplified using primers Ph2-F1 (5'-AAGCTTATGTCCGGGCACCTC

CA-3') and Ph2-R1 (5'-CICGAGTCTGCATATTCATTCCA-3') with added HindIII and XhoI restriction sites underlined. The amplified fragment was then cloned into the p2T7-PhB construct already containing the PHB1 gene, resulting in a construct containing juxtaposed fragments of the PHB1 and PHB2 genes, located amongst the opposing inducible T7 promoters.

### 2.3. Electroporation, cloning and growth curves

All three constructs were electroporated into procyclic form *T. brucei* strain 29-13 and cell clones were obtained following a protocol described elsewhere (Vondrušková et al., 2005). Synthesis of double stranded (ds) RNA was induced by the addition of 1 µg/ml tetracycline. Growth curves of parental, non-induced and RNAi-induced cell lines were obtained using the Beckman Z2 Coulter over a period of 12 days.

### 2.4. Northern blot analysis

For Northern blot analysis, ~10 µg per lane of total RNA from procyclic cells was separated in a 1% formaldehyde agarose gel, blotted and cross-linked as published elsewhere (Vondrušková et al., 2005). After pre-hybridization in NaPi solution (0.25 M Na<sub>2</sub>HPO<sub>4</sub> and 0.25 M NaH<sub>2</sub>PO<sub>4</sub>, pH 7.2, 1 mM EDTA, 7% SDS) for 2 h at 55 °C, hybridization was performed overnight in the same solution at 55 °C. A wash in 2× saline sodium citrate solution (SSC), 0.1% SDS at room temperature (RT) for 20 min was followed by two washes in 0.2× SSC, 0.1% SDS for 20 min each at 55 °C.

### 2.5. Generation of antibodies and Western blot analysis

Affinity purified polyclonal antibodies against PHB1 were raised against a synthetic oligopeptide by Alpha Diagnostic International, Inc. (San Antonio, USA). The oligopeptide used corresponds to the 201–219 amino acid region of the *T. brucei* protein. For Western blot analyses, cell lysates of the *T. brucei* parental strain, non-induced and induced clonal cell lines corresponding to 5 × 10<sup>6</sup> procyclic cells/lane were separated on a 12% SDS–PAGE gel. The polyclonal rabbit antibodies against PHB1, mitochondrial RNA-binding protein 1 (MRP1) (Vondrušková et al., 2005; Zíková et al., 2006), guide RNA-binding protein 1 (GAP1) (Hashimi et al., 2009), trypanosome-specific subunit 4 of cytochrome oxidase (trCOIV), Fe–S cluster scaffold protein 1 (IscU) (Smíd et al., 2006) and frataxin (Long et al., 2008) were used at 1:1,000, 1:1,000, 1:500, 1:1,000 and 1:1,000 dilutions, respectively. Additional antibodies against terminal alternative oxidase (TAO) (provided by G.C. Hill, Vanderbilt University School of Medicine, USA), heat shock protein 60 (hsp60) and apocytochrome c<sub>1</sub> (provided by S.L. Hajduk, University of Georgia, USA), and antibodies generated against the entire F<sub>1</sub> moiety of ATP synthase (ATPase) from *Crithidia fasciculata* (provided by R. Benne, University of Amsterdam, Netherlands), were used at 1:1,000, 1:100 and 1:10,000 and 1:1,000 dilutions, respectively.

### 2.6. Cell fractionation

Digitonin fractionation was performed as described elsewhere (Smíd et al., 2006). The mitochondrial vesicles from 5 × 10<sup>8</sup> cells were isolated by hypotonic lysis as described previously (Horváth et al., 2005). Pelleted mitochondrial vesicles were stored at –80 °C until further use. Alternatively, crude mitochondrial pellet obtained by digitonin treatment described above was loaded on a Percoll gradient. After ultracentrifugation, the mitochondrial fraction was isolated following the protocol published elsewhere (Schneider et al., 2007).

### 2.7. Measurement of respiration, reactive oxygen species (ROS) and membrane potential

Exponentially growing cells at concentration 5 × 10<sup>6</sup> cell/ml were spun (800 g for 5 min), washed, and resuspended in 1 ml of fresh semi-defined media (SDM)-79 cultivation medium at a concentration of 3 × 10<sup>7</sup> cell/ml. Oxygen consumption was determined with a Clark electrode (Strathkelvin). At 4 min intervals, KCN and salicylhydroxamic acid (SHAM) were added to final concentrations of 0.1 and 0.03 mM, respectively.

For the measurement of free ROS, exponentially growing cells were resuspended in fresh SDM-79 medium at a concentration 5 × 10<sup>6</sup> cell/ml and dihydroethidium was added to final concentration 5 µg/ml. Cells were incubated at 27 °C for 30 min and then transferred into isoflow. Free radicals were detected by an Epics XL flow cytometer (Beckman Coulter) with excitation and emission settings of 488 nm and 620 nm. Tetramethylrhodamine ethyl ester (TMRE) (Molecular Probes) uptake was used as a measure of the mitochondrial membrane potential as described elsewhere (Long et al., 2008).

### 2.8. Blue-native electrophoresis

Analysis of the PHB complex was performed by one (1D) or two-dimensional (2D) blue native/Tricine–SDS–PAGE gels as described previously (Horváth et al., 2002; Neboháčová et al., 2005). For 1D electrophoresis, 50 or 100 µg of proteins from the mitochondrial lysate, isolated by hypotonic lysis from ~1 × 10<sup>7</sup> procyclic cells, was mixed with 1.5 µl of CB solution (0.5 M ε-amino-*n*-caproic acid, 5% (w/v) Coomassie brilliant blue G-25), incubated for 10 min on ice and resolved on 2–15% gradient blue native gel.

For 2D electrophoresis, 100 µg of mitochondrial lysate prepared as described above was analysed on 2–15% gradient blue native and 12% Tricine–SDS–PAGE gels. After electrophoresis, the gels were blotted and probed with the anti-MRP1 (1:1,000) (Vondrušková et al., 2005) and anti-PHB1 polyclonal antibodies (1:1,000) (prepared as described above) and secondary anti-rabbit antibodies (1:1,000) (Sevapharma, Prague, Czech Republic). Secondary antibodies coupled with horseradish peroxidase were visualised according to the manufacturer's protocol using the ECL plus kit (Amersham Biosciences, Chalfont St. Giles, UK).

### 2.9. Fluorescence and electron microscopy

Cells in logarithmic phase were harvested and stained with Mitotracker Red CMX (Molecular Probes), followed by fixation and staining with DAPI as described elsewhere (Long et al., 2008). Cells were imaged using an Olympus IX81 microscope and images were captured using an Orca-AG digital camera and cellR imaging software.

For transmission electron microscopy, procyclic cells were washed in 0.1 M PBS and fixed in 2.5% (v/v) glutaraldehyde in 0.1 M sodium cacodylate (SC) buffer, pH 7.4, for 1 h at 4 °C. After a quick wash in the SC buffer, they were postfixed with 2% (w/v) osmium tetroxide in the SC buffer for 1 h at room temperature. After dehydration in ethanol, the cells were embedded in Epon-Araldite, and thin sections stained with lead citrate and uranyl acetate were examined under a JEOL JEM 1010 microscope.

### 2.10. Mitochondrial protein synthesis in vivo

Analysis of de novo mitochondrial translation followed procedures described previously (Horváth et al., 2002; Neboháčová et al., 2005). In brief, 5 × 10<sup>7</sup> exponentially growing cells were pelleted by centrifugation at 2,000 g for 10 min, washed twice and resuspended in 100 µl of the SoTE buffer (0.6 M sorbitol, 20 mM

Tris-HCl, pH 7.5, 2 mM EDTA). Mitochondrial translation products were labelled by incubating whole cells ( $5 \times 10^7$  procyclic form cells) for 2 h at 27 °C in the presence of EasyTag™ EXPRESS<sup>35S</sup> protein labelling mix (100  $\mu$ Ci per 100  $\mu$ l reaction) with the concurrent inhibition of the cytosolic translation by 100  $\mu$ g/ml cycloheximide. The labelled cells were extracted with Triton X-100 to remove soluble proteins and the remaining hydrophobic material was analysed in denaturing 2D (9.5% versus 15%) polyacrylamide Tris-glycine SDS gels as described previously (Horváth et al., 2002).

### 3. Results

#### 3.1. Genes coding for PHB1 and PHB2

The *T. brucei* genome contains single copies of PHB1 (Tb927.8.4810) and PHB2 (Tb10.70.2920), with calculated molecular masses of 31.5 kDa and 32.0 kDa, respectively. The gene sequences

show only 34% identity. The PHB1 and PHB2 homologues are also present in the genomes of the other investigated trypanosomatids (*T. cruzi*, *L. infantum*, *L. major* and *L. braziliensis*) ([www.genedb.org](http://www.genedb.org)). Comparisons of the deduced amino acid sequences of the trypanosomatid PHBs with their homologues from selected eukaryotes revealed identity levels ranging between 40% and 45% for PHB1 and 35–40% for PHB2. Each single-copy gene possesses a characteristic PHB Smart domain (overlapping with the Band 7 Pfam domain) and a single predicted transmembrane helix in the N-terminal region. The probability of mitochondrial localisation is only 0.66 for PHB1 and 0.46 for PHB2 by the mt import signal prediction programme Mitoprot, but such relatively low values are not uncommon for mitochondrial proteins in trypanosomatids, and only indicate that protein sorting rules that operate in these organisms have not been fully accounted for.

The phylogenetic relationships of trypanosomatid PHBs with their counterparts from several representative eukaryotes were investigated by a minimal evolutionary analysis of the protein se-

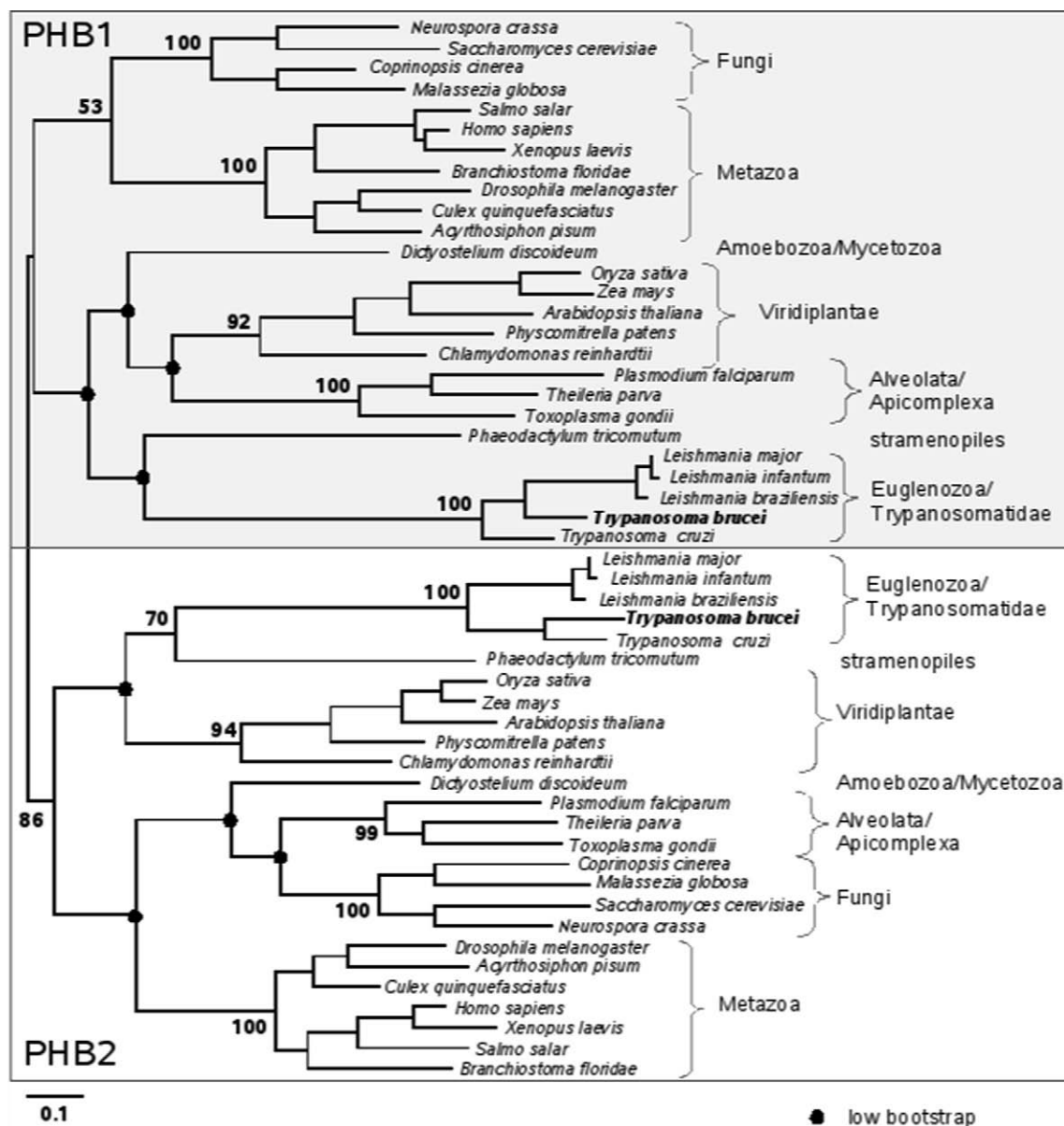


**Fig. 1.** Minimal evolutionary phylogenetic tree of the eukaryotic prohibitin (PHB) family. The alignment was generated using Clustal X (version 2.0.10). The unalignable N-terminal and C-terminal regions of the proteins, as well as several internal indel positions, were manually removed, and the remaining alignment containing 207 positions was subjected to minimal evolution analysis with bootstrap (1,000 replicates) using MEGA (version 4). The Dayhoff PAM matrix of amino acid substitution was used and variable sites were assumed to follow  $\gamma$ -distribution. The tree is unrooted.

quences. The tree (Fig. 1) shows that all PHBs fall into two major clades representing the PHB1 and PHB2 sub-groups from each taxon included. This topology is consistent with the notion that separation of the PHB sub-groups predates diversification within eukaryotes. The tree also shows that within each sub-group, trypanosomatid proteins are amongst the most diverged from the remaining eukaryotes. Although the details of topology are different for the PHB1 and the PHB2 sub-trees, the major groups of eukaryotes included in the alignment (Euglenozoa, Metazoa, Fungi, Plants, Apicomplexa) have been recovered with a high bootstrap support. The deep branching order is poorly supported, but that is a common problem for eukaryotic trees (Keeling et al., 2005; Brinkmann and Philippe, 2007). Overall, the analysis confirms the identification of the prohibitins from *T. brucei* and other trypanosomatids as members of the PHB1 and PHB2 protein sub-families.

### 3.2. Loss of PHB1 is lethal

Due to frequently encountered problems with RNAi 'leakage' or incomplete ablation, we prepared two different RNAi cell lines for the down-regulation of PHB1. The first is based on the p2T7-177 vector equipped with opposing regulatable promoters (PHB1-177 cells), whilst the second cell line contains the pLew100 vector, which supports the synthesis of dsRNA from a single promoter (PHB1-100 cells). Growth inhibition of both cell lines becomes apparent 6 days after the induction of RNAi silencing (Fig. 2A and B). Thereafter, the growth of induced cells virtually stops, and this lasts until day 12 when the growth is resumed to a limited extent, probably due to developed resistance to RNAi. Northern blot analyses of total RNA from parental 29-13 cells with a probe derived from the coding region of PHB1 detected abundant mRNA. Comparison between the non-induced and RNAi-induced cells revealed elimination of most of the targeted transcript within 48 h of induction (Fig. 2A and B; insets).

Considering the doubling time of *T. brucei* procyclic cells to be approximately 8 h, the growth inhibition observed in each PHB1 RNAi-induced cell line is rather delayed compared with knock-down cells for other mitochondrial proteins in *T. brucei* (Vondrušková et al., 2005; Horváth et al., 2005; Smíd et al., 2006; Long et al., 2008). We wondered whether the other component

of the PHB complex, PHB2, is responsible for this effect. Therefore, we prepared cell lines, in which both PHB transcripts were eliminated (PHB1 + 2). Northern blot analyses of total RNA isolated from these non-induced and RNAi-induced cells hybridized with probes against the PHB1 and PHB2 genes confirmed tandem elimination of both transcripts (Fig. 2C; inset). However, targeting of both PHBs did not accelerate the onset of the reduced growth phenotype, as a significant growth decrease also occurred, only at day 6 (Fig. 2C). The double knock-down cells did not become refractive to RNAi even 24 days after induction (data not shown).

As our attempt to obtain antibodies against the full-size PHB1 protein over-expressed in *Escherichia coli* failed, and the tested antibodies against yeast PHB1 did not cross-react with its trypanosome homologue, we used rabbit polyclonal antibodies raised against the oligopeptide derived from the *T. brucei* PHB1 amino acid sequence. Western analyses of the total cell lysates of the induced double knock-down cells (in contrast to the non-induced cells and parental cells) showed a rapid decrease in the PHB1 protein, with its total elimination by day 4 (Fig. 3A). A similar situation was observed in the single knock-down cell lines (see below and data not shown).

### 3.3. PHB1 is confined to the mitochondrion

As PHBs were found in various compartments of yeast and human cells (Merkwirth and Langer, 2009), we examined localisation of the PHB1 protein in *T. brucei*. Total cell lysates and sub-cellular fractions obtained with digitonin treatment were immunoprobed with anti-PHB1 antibodies, as well as with antibodies against marker mitochondrial and cytosolic proteins. The target protein was abundant in the mitochondrion, whereas no signal was observed in the cytosol (Fig. 3B). Furthermore, we have prepared highly pure mitochondrial vesicles by combining the digitonin treatment and sedimentation in Percoll gradient. Again, all PHB1 protein was confined to the organelle (Fig. 3C). Antibodies against enolase and the MRP1 protein, which are exclusively localised in the cytosol and mitochondria, respectively (Long et al., 2008; Vondrušková et al., 2005), confirmed the absence of cross-contamination of the assayed sub-cellular fractions (Fig. 3B and C).

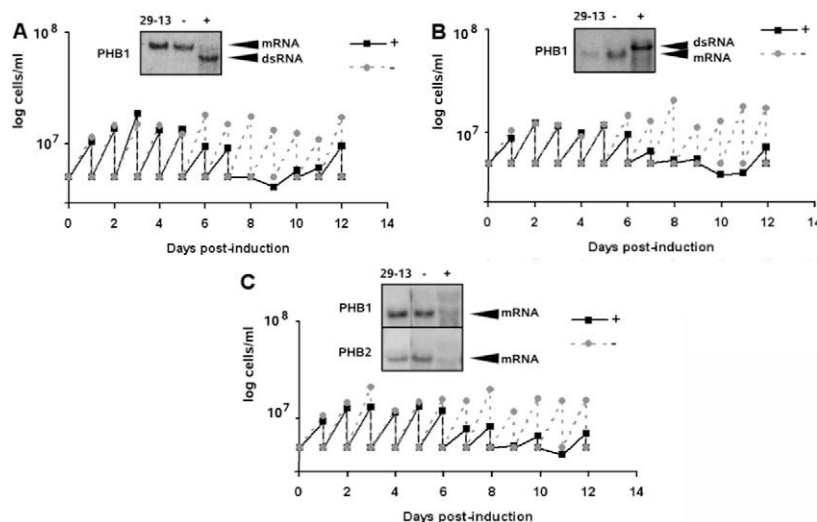


**Fig. 2.** Effect of prohibitin 1 (PHB1) and PHB1 + 2 RNA interference (RNAi) on *Trypanosoma brucei* cell growth and mRNA levels. Cell densities (cells/ml) that were measured every 24 h are plotted on a logarithmic scale on the y-axis over 12 days. Cells were diluted to  $2 \times 10^6$  cells/ml every day. Cells grown in the absence or presence of 1  $\mu$ g/ml tetracycline, the addition of which induces RNAi, are indicated by dashed (tet-) or black (tet+) lines, respectively. Growth curves of the PHB1-100 (A), PHB1-177 (B) and PHB1 + 2 (C) clonal cell lines are shown. The insets show a Northern blot analysis of the total RNA extracted from the parental 29-13 cells (lane 1), non-induced RNAi cells (lane 2) and respective induced RNAi cells (lane 3). In (A and B), the 525 nucleotide long 5' region of the PHB1 gene was used as a probe. In the inset panels of C, 5' regions of the PHB1 and PHB2 genes (410 nucleotides long) were used as probes, respectively, as labelled.

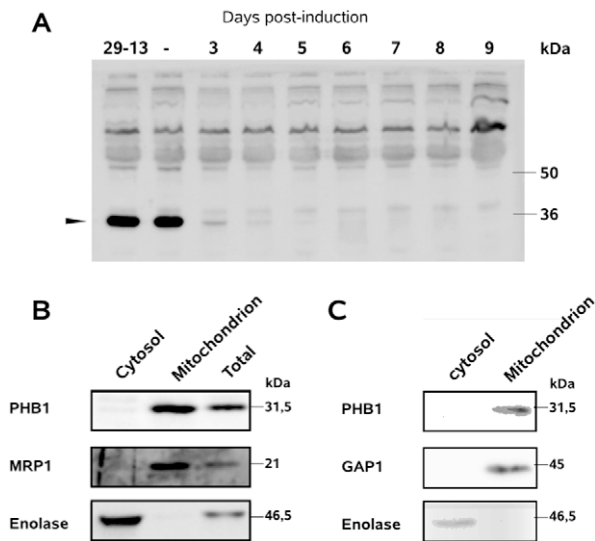


**Fig. 3.** Mitochondrion-confined prohibitin 1 (PHB1) is eliminated upon RNA interference (RNAi) induction. The PHB1 protein level was analysed by Western blot analysis in extracts from *Trypanosoma brucei* parental 29-13 cells, non-induced PHB1+2 double knock-down cells, and cells at days 3–9 post-induction. Non-specific reactivity bands in the upper part of the gel serve as a loading control (A). (B) Western blot analysis of the expression of the PHB1 protein in cytosolic and mitochondrial fractions isolated by digitonin extraction, as well as in the total cell lysate of procyclic *T. brucei*. Mitochondrial RNA-binding protein 1 (MRP1) and enolase were used as mitochondrial and cytosolic markers, respectively. (C) Western blot analysis of the expression of the PHB1 protein in cytosolic and mitochondrial fractions of procyclic *T. brucei*. Mitochondrial vesicles were isolated by digitonin extraction followed by Percoll gradient centrifugation. Guide RNA-binding protein 1 (GAP1) and enolase were used as mitochondrial and cytosolic markers, respectively.

### 3.4. PHB1 is part of a large complex

PHBs in yeast and human mitochondria have been shown to form a large supramolecular protein complex (Nijtmans et al., 2000; Tatsuta et al., 2005). In order to check whether a similar situation exists in the divergent protist under study, mitochondrial lysate obtained from parental 29-13 cells by hypotonic lysis was analysed using a 2D blue native/Tricine-SDS-PAGE gel followed by immunoprobining with anti-PHB1 antibodies. A mitochondrial 100 kDa MRP1/2 complex was used for comparison (Schumacher et al., 2006). By comparing the position of the ~31 kDa PHB1 signal with that of the 21 kDa MRP1 protein, we concluded that PHB1 is part of a complex that is substantially larger than MRP1/2 (Fig. 4).

In order to establish its size, we used 1D blue native gels, upon which varying amounts of mitochondrial protein were loaded, blotted and probed with anti-PHB1 antibodies. As shown in Fig. 5A, a single strong band was detected that represented a complex migrating much slower than the 880 kDa marker. Based on its mobility in several gels (data not shown), we estimate that in *T. brucei* the PHB complex is ~1.5 MDa in size. Furthermore, we used blue native gel analyses to investigate the effect of PHB1 RNAi on this complex. As shown in Fig. 5B, both in the single PHB1 and the double PHB1+2 RNAi knock-down experiments, at 5 days post-induction, virtually all complex-bound PHB1 was eliminated.

### 3.5. Effect on mitochondrial translation

Since PHBs in yeast were functionally associated with mitochondrial translation, we decided to examine the effect of PHB1+2 RNAi ablation on de novo organellar protein synthesis in *T. brucei*. Due to their extreme hydrophobicity, it is quite challenging to visualise products of mitochondrial translation in try-

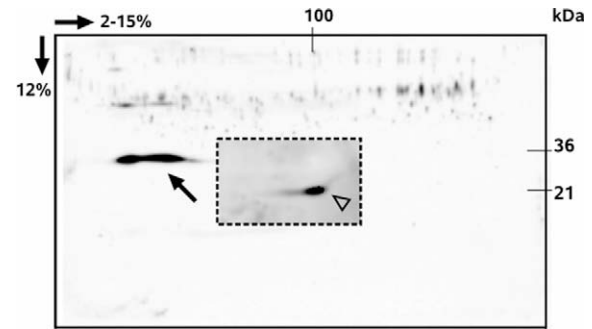


**Fig. 4.** Prohibitin 1 (PHB1) is present in a complex. Proteins from purified mitochondria were resolved in two-dimensional 2–15% gradient blue-native/12% Tricine SDS-PAGE gels. Parallel gels were blotted and probed with the anti-mitochondrial RNA-binding protein 1 (MRP1) (inset) and anti-PHB1 antibodies. Localisation of the PHB1 and MRP1 proteins is indicated by an arrow and arrowhead, respectively. The 21 kDa MRP1 protein present in the 100 kDa MRP1/2 complex (Schumacher et al., 2006) was used as a marker for the second dimension. The positions of molecular mass markers are indicated on the right and at the top.

panosomes, which tend to aggregate and display an aberrant mobility in electrophoretic SDS gels (Horváth et al., 2000). The latter property was utilised to devise a special 2D electrophoretic procedure that allowed detection of such proteins in the characteristic off-diagonal positions in the gel (Horváth et al., 2000, 2002).

When the non-induced *T. brucei* procyclic cells were subjected to the in vivo labelling assay in the presence of cycloheximide, an inhibitor of cytosolic translation, and the labelled proteins were separated in the 2D polyacrylamide-SDS gel, we detected discrete labelled spots off the main diagonal (Fig. 6A). These spots could be correlated with the known positions of monomeric and aggregated forms of cytochrome c oxidase subunit I (co1) and apocytochrome b (cyB), testifying for organellar translation under these conditions.

Next, the PHB1+2 knock-down cells 2 or 3 days post-RNAi-induction were subjected to an in vivo labelling assay. Whilst no change in the labelling pattern was observed at the earlier time-point (data not shown), at day 3 both co1 and cyB disappeared (Fig. 6B). Moreover, the in vivo translated proteins did not appear in the lysates of PHB1 cells after 5 days of RNAi induction (data not shown), confirming that mitochondrial translation is shut down in the absence of PHBs.

### 3.6. Nuclear-encoded mitochondrial proteins and ROS are unaltered, but mitochondrial membrane potential is decreased

Results obtained with yeast cells indicate that the PHB complex is closely associated with complex V (Osman et al., 2007) and may possibly interact with other proteins and/or protein complexes, therefore we investigated the effect of PHB1 RNAi on mitochondrial respiration-related properties. First, we followed the steady-state levels of selected mitochondrial proteins in *T. brucei* cells depleted for PHB1 (Fig. 7). Remarkably, the repression of PHB1 did not result in a detectable loss of ATPase, as judged using polyclonal antibodies generated against the entire ATPase complex. Moreover, levels of subunits of respiratory complexes III (apocytochrome c<sub>1</sub>) and IV (trypanosome-specific cytochrome oxidase subunit IV), Fe–S cluster assembly proteins IscU and frataxin, and the RNA-binding protein MRP1 remained unaltered. Similarly, the levels of two assayed mitochondrial matrix proteins, the TAO and hsp60 were also not affected (Fig. 7).

Next, we measured mitochondrial inner membrane potential by quantifying the uptake of TMRE. Whilst no change was observed in the non-induced cells compared with the parental cells, membrane potential dramatically decreased in the single or double knock-

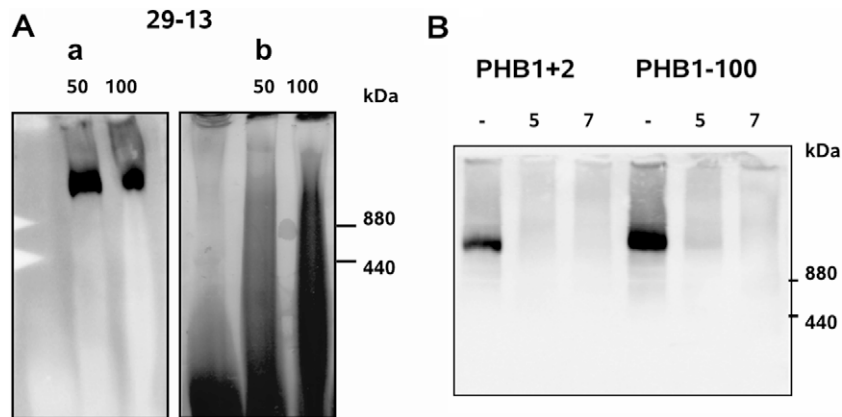


**Fig. 5.** Prohibitin 1 and 2 (PHB1 + 2) is present in an ~1.5 MDa complex. (A) The level of PHB1 protein was analyzed by Western blot analysis in mitochondrial lysates from *Trypanosoma brucei* 29-13 cells using PHB1 antibody. Protein amounts of 50 and 100 µg (indicated on top) were resolved on a single dimension 2–15% blue native gel and subjected to Western analysis (a), and is shown before transfer (b). The positions of molecular mass markers are indicated on the right (monomer and dimer of ferritin (Sigma)). (B) The presence of PHB1 in non-induced cells PHB1 + 2 (–) and PHB1–100 (–) and its elimination by RNA interference (RNAi) as confirmed by Western blots of mitochondrial lysates taken at days 5 and 7 after induction of RNAi.

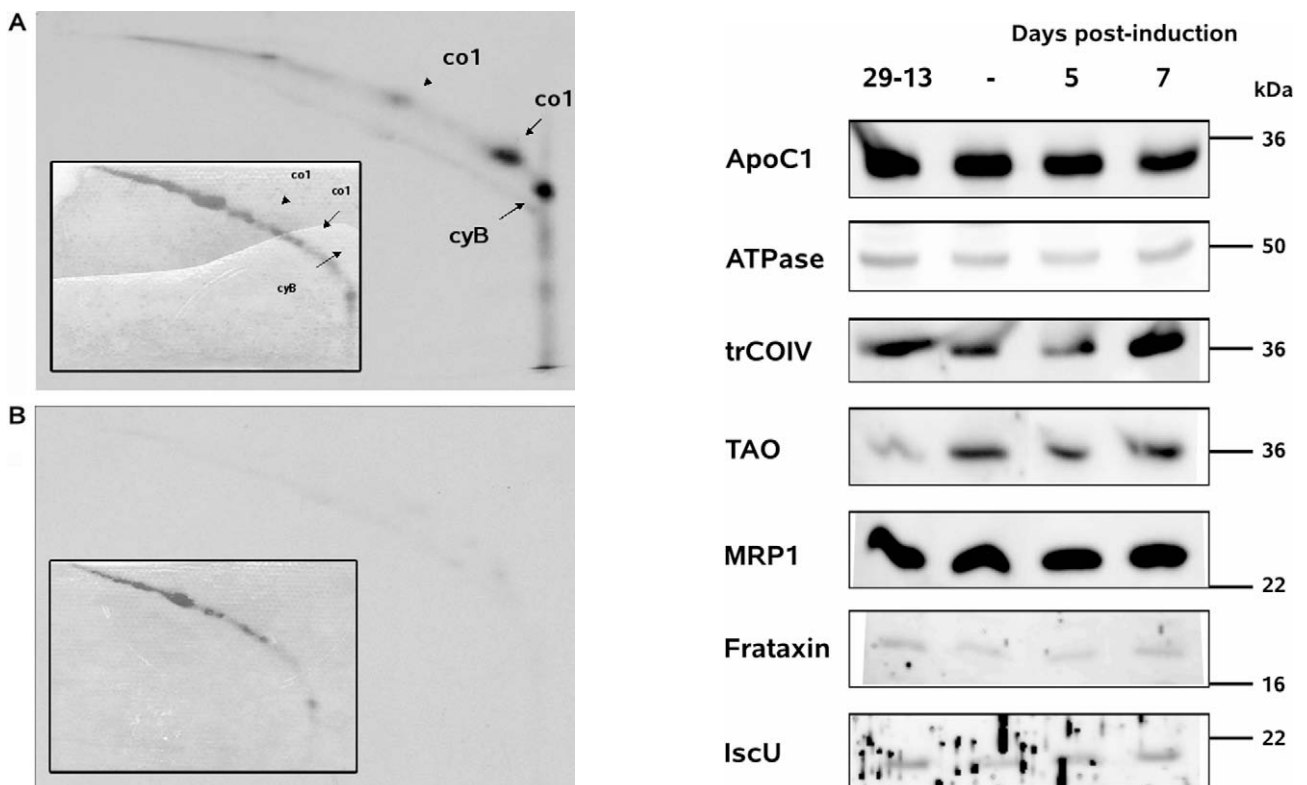


**Fig. 6.** Mitochondrial translation is shut down in the absence of prohibitins (PHBs). Isolated mitochondrial fractions from PHB1 + 2 non-induced cells (A) and after 3 days of RNA interference (RNAi) induction (B) were extracted with 0.05% Triton X-100 and resolved in 9.5% versus 15% two-dimensional polyacrylamide Tris–glycine SDS gels, stained and visualised as described in Section 2. De novo synthesised cytochrome oxidase subunit I (co1) and cytochrome *b* (cyB), pulse-labelled with EasyTag™ EXPRESS<sup>35</sup>S protein labelling mix, are marked with arrows. Inset shows the same gels stained with Coomassie brilliant blue R250.

down cells. The decrease was, however, somewhat delayed, as it appeared at day 5 post-induction (data not shown) and became massive 2 days later (Fig. 8A–C).

Finally, using dihydroethidium, we measured the accumulation of ROS, as its increase was associated with PHB deficiency in human cells (Schleicher et al., 2008). However, no significant difference in the levels of ROS between the non-induced and induced

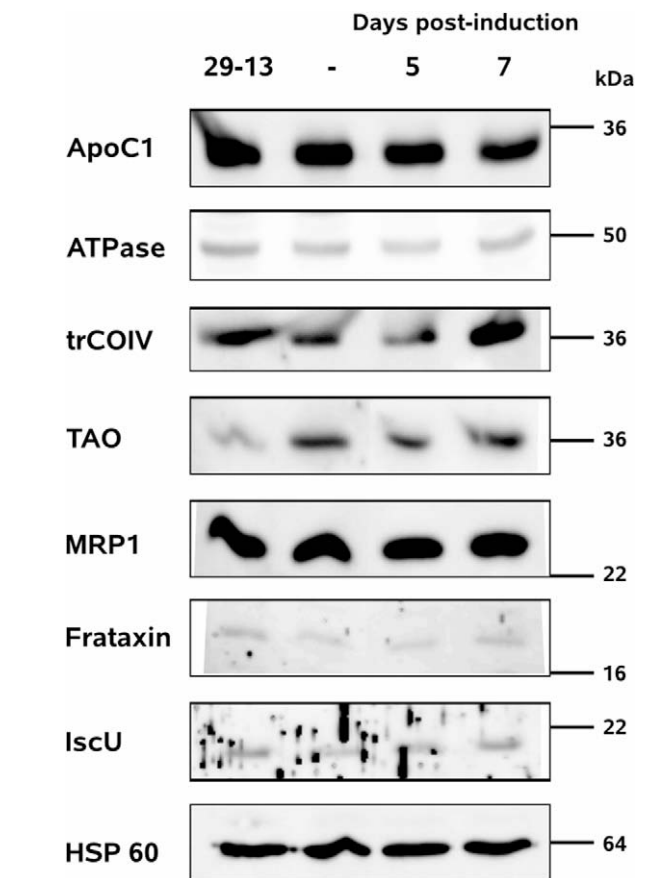


**Fig. 7.** The abundance of assayed mitochondrial proteins is not altered in the absence of prohibitin 1 (PHB1). Expression levels of apocytochrome *c*<sub>1</sub> (apoC1), F<sub>1</sub> moiety of ATP synthase (ATPase), trypanosome-specific subunit 4 of cytochrome oxidase (trCOIV), terminal alternative oxidase (TAO), mitochondrial RNA-binding protein 1 (MRP1), Fe–S cluster scaffold protein (IscU), frataxin (Frax) and heat shock protein 60 (hsp60) as determined by immunoblot analysis of whole cell lysates of *Trypanosoma brucei* parental 29-13 cells (wt), and the PHB1 + 2 knock-down cells both before (–) and after 5 and 7 days of RNA interference (RNAi) induction.

cells was observed (Fig. 8D and data not shown). The accumulation of ROS in the *T. brucei* cells ablated for frataxin (Long et al., 2008) was used as a control (data not shown).

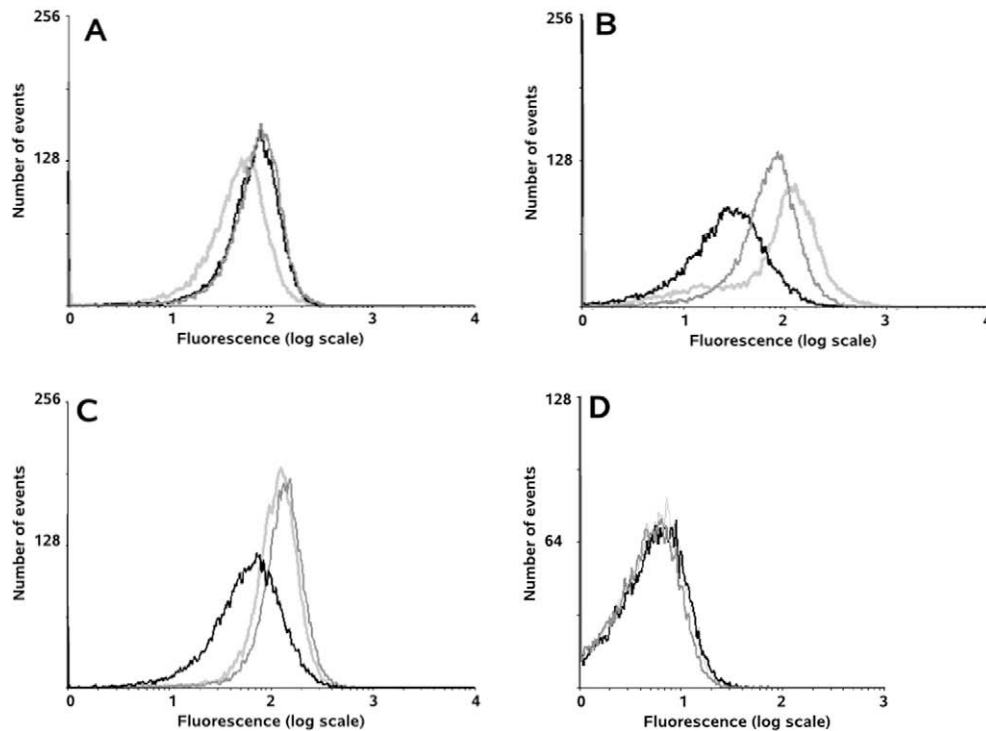


**Fig. 8.** Mitochondrial membrane potential but not reactive oxygen species (ROS) is altered in all RNA interference (RNAi) induced prohibitin (PHB) knock-down cells. Inner membrane potential was measured by flow cytometry following incubation of cells with 0.4% tetramethylrodamine ethyl ester (TMRE) for 20 min, and fluorescence distributions were plotted as frequency histograms. *Trypanosoma brucei* parental 29-13, non-induced and RNAi-induced PHB1 + 2 cells 3 days post-induction (A), 5 days post-induction (B) and 7 days post-induction (C) are shown in light grey, grey and black lines, respectively. The presence of ROS was measured in cells incubated in the presence of 5  $\mu$ g/ml dihydroethidium for 30 min and analysed by flow cytometry. As an example, the measurements of parental 29-13, non-induced and RNAi-induced PHB1 + 2 cells (5 days after RNAi induction) are shown in light grey, grey and black lines, respectively (Fig. 8D).

### 3.7. Mitochondrial morphology is altered

In murine cells, PHB2 is required for normal mitochondrial morphology (Merkwirth et al., 2008), therefore we have investigated whether the related function is observed in *T. brucei*. Non-induced and RNAi-induced single and double knock-down cells were stained with the membrane potential-dependent Mitotracker Red and analysed by fluorescence microscopy. In parental and non-induced cells the staining revealed the characteristic pattern of a single tubular and reticulated mitochondrion (Fig. 9B and E). However, in the RNAi-induced cells (Fig. 9H and data not shown) the mitochondrial tubules were substantially extended in some areas. As shown by differential interference contrast, cellular integrity is retained in all analysed cells (Fig. 9C, F and I). DAPI staining allows easy tracking of the huge mitochondrial DNA network, termed kinetoplast (k) DNA, which is arranged in a highly compacted disk in *T. brucei*. The integrity of the kDNA seems to be preserved in all investigated cells (Fig. 9A, D and G).

In order to better reveal the alterations present in cells ablated for PHB1, we used transmission electron microscopy. In all cell lines, the loss of PHB1 triggered significant morphological changes of the single elongated and reticulated mitochondrion. At day 5 post-RNAi induction, the PHB1 knock-down cells (pLew100-PhA) featured an enlarged organelle that had lower electron density (Fig. 10C and E) compared with the parental 29-13 strain (data not shown) and the non-induced PHB1 + 2 cells (Fig. 10A and B). A similar result was observed in the p2T7-PhB cells, in which PHB1 was ablated using a different construct (Fig. 10D). The inflation of the mitochondrion was even more pronounced in the double knock-down cells at days 5 and 7 of RNAi induction (Fig. 10F and G). It is worth noting, however, that the electron dense kinetoplast, containing all mitochondrial DNA, remained unaltered in sin-

gle and double knock-down cells at 5 and 7 days of induction, and retained its specific position close to the basal body of the flagellum (Fig. 10C, D, G and I). Similarly, the short inconspicuous tubular cristae did not disappear from the significantly altered organelle, but were displaced to its periphery (Fig. 10H). In the PHB1 + 2 cells the kDNA network not only retained its wild-type morphology and periflagellar position even 7 days post-induction, but unilateral filaments were also fully preserved in the kinetoflagellar zone (Fig. 10I). Moreover, increased electron density at the antipodal sites of the disk confirms the retention of the two protein centres, organizing replication of the kDNA. All other cellular structures such as the nucleus, nucleolus, lipid droplets, endoplasmic reticulum, flagellum, acidocalcisomes and the corset of subpellicular microtubules appear to be unaltered following the loss of either PHB1 (Fig. 10C and D) or PHB1 + 2 (Fig. 10G).

## 4. Discussion

To date, the function of PHB has only been studied in the mitochondrion of model organisms, such as *S. cerevisiae*, *C. elegans* and mammals (Ikonen et al., 1995; Nijtmans et al., 2000; Artal-Sanz et al., 2003; Merkwirth et al., 2008; Schleicher et al., 2008). However, all of them belong to the supergroup Unikonta, comprising only a fraction of currently recognised eukaryotic diversity (Keeling et al., 2005). Therefore, our understanding of the evolution and functional diversity of this omnipresent protein is restricted to this group of organisms. One possibility to gain further insight into the functions of PHBs, and to address which of those are primary and which arose later in evolution, is to study their roles in representatives of other major groups, as we do here in *T. brucei*. This parasitic protist is the most genetically tractable representative of the early-branching Excavata. Our phylogenetic analysis of

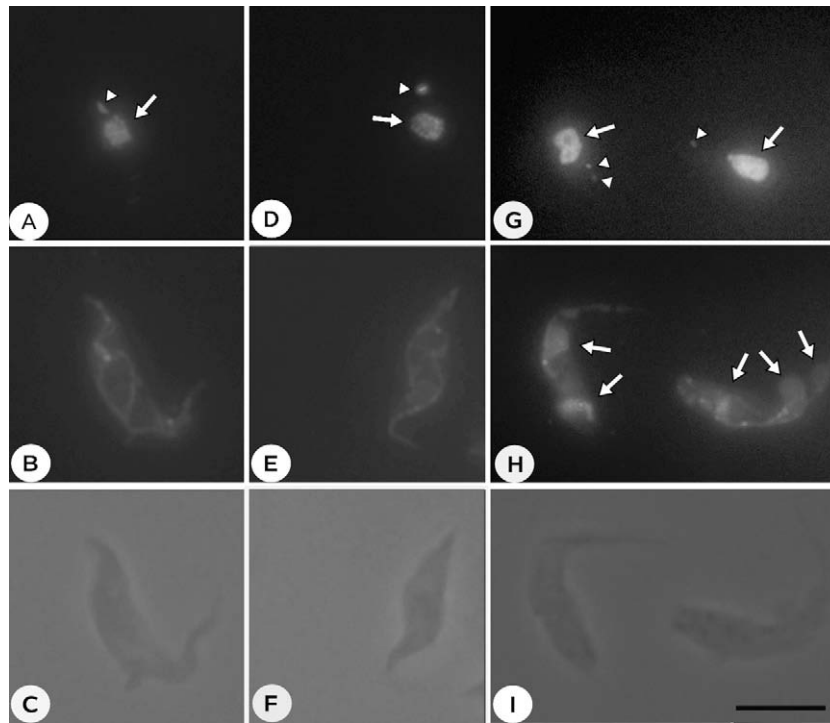


**Fig. 9.** Light microscopy reveals the integrity of mitochondrial (=kinetoplast) DNA in all examined cells and an extension of the mitochondrion in RNA interference (RNAi)-induced cells. *Trypanosoma brucei* parental 29-13 (A–C), non-induced (D–F) and RNAi-induced PHB1 + 2 cells (G–I) were stained with DAPI (A, D and G) and Mitotracker Red (B, E and H), and were viewed using differential interference contrast (C, F and I). Arrowheads and arrows indicate kinetoplast and nDNA, respectively (A, D and G). In (H), the arrow points to the extended region of the mitochondrion. Scale bar = 10  $\mu$ m.

PHBs from several major groups of eukaryotes showed that the trypanosome homologues are indeed found amongst the most diverged members of the family.

Since in multicellular organisms, PHBs were found in various cellular compartments, we first addressed intracellular distribution of PHB1 in *T. brucei*. All of the protein seems to be confined to the single reticulated mitochondrion, forming a very large protein complex, the proper function of which is essential for survival of these flagellates. This indicates that evolutionary ancestral localisation of PHBs is within this organelle and that they were likely inherited by the proto-eukaryote from an engulfed  $\alpha$ -proteobacterium. Further corroborating the recently proven dependence of cell proliferation on mitochondrial-located PHBs in mammals, we found no evidence for non-mitochondrial functions of these proteins in trypanosomes.

As the growth phenotype of the single and double knock-down cells is similar, we assume that as in other eukaryotes, both proteins are mutually dependent and essential subunits of the heteromeric PHB complex, the size of which we estimate to be  $\sim$ 1.5 MDa in *T. brucei*. Two phenotypic consequences of the PHB1 ablation in trypanosomes appear to be primary, namely the alteration of mitochondrial morphology and the impact on mitochondrial translation.

By virtue of the large size of its mtDNA, here termed the kDNA, *T. brucei* and other trypanosomatids are particularly useful for studying phenotypes associated with organellar DNA. This enabled us to directly follow the size and localisation of the kDNA in knock-down cells at several time-points after RNAi induction. As in mammals and *C. elegans* (Artal-Sanz et al., 2003; Kasashima et al., 2006; Merkwirth et al., 2008), mitochondrial morphology undergoes dramatic changes, including a substantial increase in organellar volume, resembling inflation, early after the ablation of PHB1 in single or double knock-down cells. Unexpectedly, however, there is no obvious effect on the kDNA network itself, as the kDNA not

only retains its disk-like packaging in the otherwise morphologically altered mitochondrion, but is also found in its specific periflagellar position with preserved fine structure, represented by the unilateral filaments in the kinetoflagellar zone (Gluznig et al., 2007). Even at day 7, when PHB1 has been fully depleted for several generations, the kDNA is present and retains its ultrastructure and position within the organelle. Therefore, we argue that the effect on mtDNA described in human cells (Kasashima et al., 2008) upon elimination of PHBs, is either secondary or has been acquired late in eukaryotic evolution. Further indirect support for the association between PHBs and mtDNA is provided by the abundance of PHB1 in yeast petite mutants lacking the organellar DNA (Nijtmans et al., 2000).

Based on studies in yeast, the PHB complex was proposed to have a direct role in respiratory chain enzyme processing as a chaperone/holdase that assists with polypeptide folding (Nijtmans et al., 2000). Indeed, our data support this function, since a rapid inhibition of mitochondrial protein synthesis was observed upon down-regulation of both PHBs. However, since we did not rule out any possible effect of PHB depletion on mitochondrial transcription and RNA processing, these results can only be interpreted as preliminary evidence for the role of PHB(s) in the stabilization of the de novo synthesised proteins. Additional indirect support for the effect on mitochondrial protein folding is provided by the delayed growth phenotype of the PHB knock-down cells, since the disruption of mtRNA processing results in reduced growth by day 3 post-RNAi-induction (Grams et al., 2002; Fisk et al., 2008; Hashimi et al., 2008). Thus, it is the chaperone/holdase activity of PHB in respirasome (Acín-Pérez et al., 2008) that appears to be essential. The increased sensitivity to apoptosis (Gregory-Bass et al., 2008), as well as the disruption of mitochondrial membrane potential observed in human and trypanosome cells upon the loss of PHBs (Ross et al., 2008; this work) is likely to be a consequence of its function in maintaining structural integrity of the organellar mem-

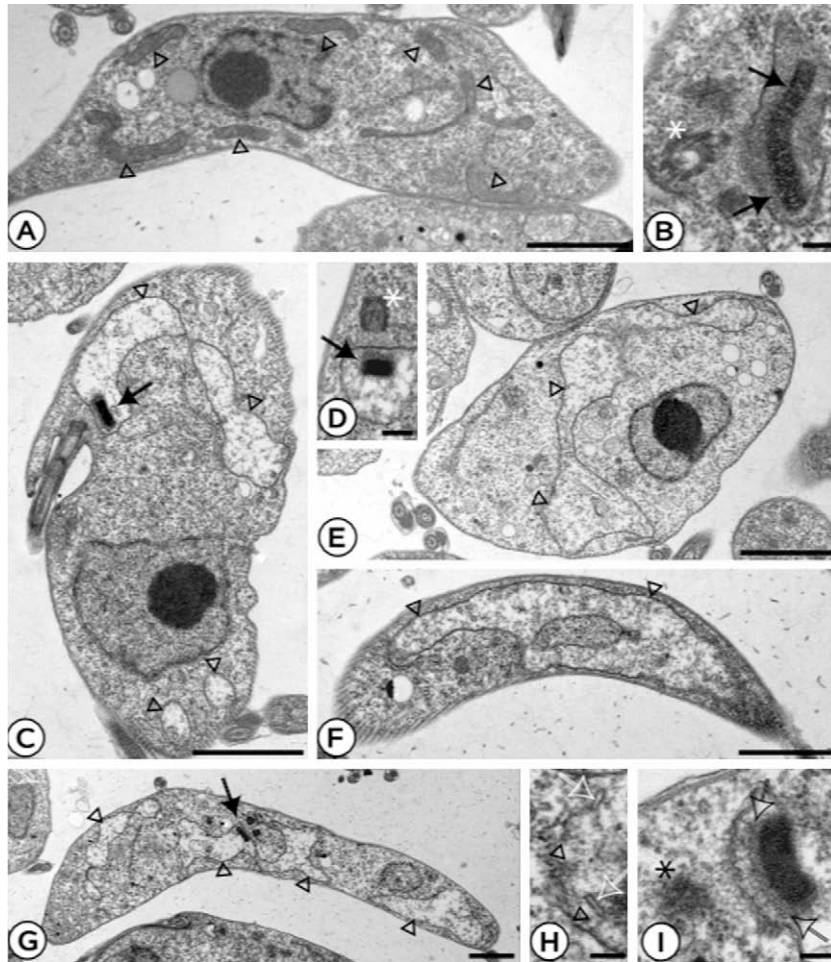


**Fig. 10.** Transmission electron microscopy of non-induced and prohibitin (PHB) RNA interference (RNAi)-induced *Trypanosoma brucei* procyclic forms. (A) Non-induced PHB1 + 2 with wild-type morphology of the single reticulated mitochondrion. Multiple cross-sections of the peripherally located organelle, its matrix being more electron dense than the cytoplasm. (B) Longitudinal section of the kinetoplast disk undergoing replication, located in the proximity of the flagellar basal body in a non-induced PHB1 + 2 cell. (C) The PHB1–100 cells after 5 days of RNAi induction, showing an enlarged mitochondrion. (D) Kinetoplast DNA retains its structure and location next to the basal body of the flagellum in PHB1–100 cells even after 7 days of RNAi. (E) The PHB1–177 cells after 7 days of RNAi induction with a mitochondrion, the contents of which have a decreased electron density. (F) Longitudinal section through the periphery of a PHB1 + 2 RNAi-induced cells 7 days post-induction revealing the massively increased volume of the mitochondrion. (G) A substantial part of the volume of this PHB1 + 2 RNAi cell 7 days post-induction is occupied by an inflated reticulated mitochondrion. The presence of the unaltered kinetoplast DNA is indicated. (H) Tubular mitochondrial cristae are shifted to the periphery of the altered organelle. (I) High magnification of the kinetoplast DNA in PHB1 + 2 cells 7 days after induction reveals that the antipodal centres and the unilateral filaments of the kinetoflagellar zone are retained even in the absence of PHB1 Arrowheads indicate mitochondrion (except in (H), where they point to the mitochondrial membrane). Filled arrows point to kinetoplast, open white arrows indicate cristae and open black arrows the antipodal centres. Flagellar basal bodies are marked by asterisks. Scale bar = 1  $\mu\text{m}$  (A, C, E, F and G), 200 nm (B, D, H and I).

brane. The exact cause of the organellar swelling is unclear. However, this may be related to the disruption of the normal cross-membrane ion traffic associated with the decrease in membrane potential.

In human epithelial cells, the loss of PHB1 results in a block of electron transport at respiratory complex I, leading to a substantial increase in mitochondrial ROS generation (Schleicher et al., 2008). The insignificant increase in ROS in *T. brucei* with down-regulated PHB1 and PHB2 can be explained by the apparent absence in this flagellate of a classical complex I (Opperdoes and Michels, 2008), to which this particular phenotypic effect of PHB has been tightly linked in other systems.

Overall, *T. brucei* proved to be a suitable model for dissecting the evolutionary conserved functions of the versatile mitochondrial protein under study. We conclude that the primary effects triggered by elimination of PHBs are the cessation of mitochondrial translation and the loss of organellar integrity. The numerous other effects described in the absence of PHBs in diverse eukaryotic cells are either secondary or have been acquired later during eukaryotic evolution.

## Acknowledgements

We thank Eva Chocholová, Alena Zíková, Pavel Poliak and Dáša Folková for their valuable contributions at an early stage of this project. The help of Anton Horváth and Petra Čermáková with 2D gels is appreciated. This work was supported by the Grant Agency of the Czech Republic 204/09/1667, the Grant Agency of the Czech Academy of Sciences A500960705, the Ministry of Education of the Czech Republic (LC07032, 2B06129 and 6007665801) and Praemium Academiae to J.L., and the Grant Agency of the Czech Republic 204/06/P423 to D.F.

## References

- Acín-Pérez, R., Fernández-Silva, P., Peleato, M.L., Pérez-Martos, A., Enriquez, J.A., 2008. Respiratory active mitochondrial supercomplexes. *Mol. Cell* 32, 529–539.
- Artal-Sanz, M., Tsang, W.Y., Willems, E.M., Grivell, L.A., Lemire, B.D., van der Spek, H., Nijtmans, L.G., 2003. The mitochondrial prohibitin complex is essential for embryonic viability and germline function in *Caenorhabditis elegans*. *J. Biol. Chem.* 278, 32091–32099.

- Berger, K.H., Yaffe, M.P., 1998. Prohibitin family members interact genetically with mitochondrial inheritance components in *Saccharomyces cerevisiae*. *Mol. Cell Biol.* 18, 4043–4052.
- Birner, R., Nebauer, R., Schneiter, R., Daum, G., 2003. Synthetic lethal interaction of the mitochondrial phosphatidylethanolamine biosynthetic machinery with the prohibitin complex of *Saccharomyces cerevisiae*. *Mol. Biol. Cell* 14, 370–383.
- Bourges, L., Ramus, C., de Camaret, B.M., Beugnot, R., Remacle, C., Cardol, P., Hofhaus, G., Issartel, J.P., 2004. Structural organization of mitochondrial human complex I: role of the ND4 and ND5 mitochondria-encoded subunits and interaction with prohibitin. *Biochem. J.* 383, 491–499.
- Brinkmann, H., Philippe, H., 2007. The diversity of eukaryotes and the root of the eukaryotic tree. *Adv. Exp. Med. Biol.* 607, 20–37.
- Coates, P.J., Jamieson, D.J., Smart, K., Prescott, A.R., Hall, P.A., 1997. The prohibitin family of mitochondrial proteins regulate replicative lifespan. *Curr. Biol.* 7, 607–610.
- Coates, P.J., Nenutil, R., McGregor, A., Picksley, S.M., Crouch, D.H., Hall, P.A., Wright, E.G., 2001. Mammalian prohibitin proteins respond to mitochondrial stress and decrease during cellular senescence. *Exp. Cell Res.* 265, 262–273.
- Fisk, J.C., Ammerman, M.L., Presnyak, V., Read, L.K., 2008. TbrGG2, an essential RNA editing accessory factor in two *Trypanosoma brucei* life cycle stages. *J. Biol. Chem.* 283, 23016–23025.
- Fusaro, G., Dasgupta, P., Rastogi, S., Joshi, B., Chellappan, S., 2003. Prohibitin induces the transcriptional activity of p53 and is exported from the nucleus upon apoptotic signaling. *J. Biol. Chem.* 278, 47853–47861.
- Gamble, S.C., Chotai, D., Odontiadiis, M., Dard, D.A., Brooke, G.N., Powell, S.M., Reebye, V., Varela-Carver, A., Kawano, Y., Waxman, J., Bevan, C.L., 2007. Prohibitin, a protein downregulated by androgens, prepresses androgen receptor activity. *Oncogene* 26, 1757–1768.
- Glueck, E., Shaw, M.K., Gull, K., 2007. Structural asymmetry and discrete nucleic acid subdomains in the *Trypanosoma brucei* kinetoplast. *Mol. Microbiol.* 64, 1529–1539.
- Grams, J., Morris, J.C., Drew, M.E., Wang, Z.F., Englund, P.T., Hajduk, S.L., 2002. A trypanosome mitochondrial RNA polymerase is required for transcription and replication. *J. Biol. Chem.* 277, 16952–16959.
- Gregory-Bass, R.C., Olatinwo, M., Xu, W., Matthews, R., Stiles, J.K., Thomas, K., Liu, D., Tsang, B., Thompson, W.E., 2008. Prohibitin silencing reverses stabilization of mitochondrial integrity and chemoresistance in ovarian cancer cells by increasing their sensitivity to apoptosis. *Int. J. Cancer* 122, 1923–1930.
- Hashimi, H., Ziková, A., Panigrahi, A.K., Stuart, K.D., Lukeš, J., 2008. TbrGG1, a component of a novel multi-protein complex involved in kinetoplastid RNA editing. *RNA* 14, 970–980.
- Hashimi, H., Čičová, Z., Novotná, L., Wen, Y.-Z., Lukeš, J., 2009. Kinetoplastid guide RNA biogenesis is dependent on subunits of the mitochondrial RNA binding complex 1 and mitochondrial RNA polymerase. *RNA* 15, 588–599.
- Horváth, A., Berry, E.A., Maslov, D.A., 2000. Translation of the edited mRNA for cytochrome *b* in trypanosome mitochondria. *Science* 287, 1639–1640.
- Horváth, A., Neboháčová, M., Lukeš, J., Maslov, D.A., 2002. Unusual polypeptide synthesis in the kinetoplastid-mitochondria from *Leishmania tarentolae*. *J. Biol. Chem.* 277, 7222–7230.
- Horváth, A., Horáková, E., Dunajčíková, P., Verner, Z., Pravdová, E., Šlapetová, I., Cuninková, L., Lukeš, J., 2005. Down-regulation of the nuclear-encoded subunits of the complexes III and IV disrupts their respective complexes but not complex I in procyclic *Trypanosoma brucei*. *Mol. Microbiol.* 58, 116–130.
- Ikonen, E., Fiedler, K., Parton, R.G., Simons, K., 1995. Prohibitin, an antiproliferative protein, is localized to mitochondria. *FEBS Lett.* 358, 273–277.
- Kasashima, K., Sumitani, M., Satoh, M., Endo, H., 2008. Human prohibitin 1 maintains the organization and stability of the mitochondrial nucleoids. *Exp. Cell Res.* 314, 988–996.
- Kasashima, K., Ohta, E., Kagawa, Y., Endo, H., 2006. Mitochondrial functions and estrogen receptor-dependent nuclear translocation of pleiotropic human prohibitin 2. *J. Biol. Chem.* 281, 36401–36410.
- Keeling, P.J., Burger, G., Durnford, D.G., Lang, B.F., Lee, R.W., Pearlman, R.E., Roger, J., Gray, M.W., 2005. The tree of eukaryotes. *Trends Ecol. Evol.* 20, 670–676.
- Larkin, M.A., Blackshields, G., Brown, N.P., Chenna, R., McGettigan, P.A., McWilliam, H., Valentin, F., Wallace, I.M., Wilm, A., Lopez, R., Thompson, J.D., Gibson, T.J., Higgins, D.G., 2007. Clustal W and Clustal X version 2.0. *Bioinformatics* 23, 2947–2948.
- Long, S., Jirků, M., Mach, J., Ginger, M.L., Sutak, R., Richardson, D., Tachezy, J., Lukeš, J., 2008. Ancestral roles of eukaryotic frataxin: mitochondrial frataxin function and heterologous expression of hydrogensomal *Trichomonas* homologs in trypanosomes. *Mol. Microbiol.* 69, 94–109.
- Manjeshwar, S., Branam, D.E., Lerner, M.R., Brackett, D.J., Jupe, E.R., 2003. Tumor suppression by the prohibitin gene 3' untranslated region RNA in human breast cancer. *Cancer Res.* 63, 5251–5256.
- McClung, J.K., Danner, D.B., Steward, D.A., Smith, J.R., Schneider, E.L., Lumpkin, C.K., Dell'Orco, R.T., Nuell, M.J., 1989. Isolation of a cDNA that hybrid selects antiproliferative mRNA from rat liver. *Biochem. Biophys. Res. Commun.* 164, 1316–1322.
- Merkwirth, C., Dargazanli, S., Tatsuta, T., Geimer, S., Lower, B., Wunderlich, F.T., von Kleist-Retzow, J.C., Waisman, A., Westermann, B., Langer, T., 2008. Prohibitins control cell proliferation and apoptosis by regulating OPA1-dependent cristae morphogenesis in mitochondria. *Genes Dev.* 22, 476–488.
- Merkwirth, C., Langer, T., 2009. Prohibitin function within mitochondria: essential roles for cell proliferation and cristae morphogenesis. *Biochim. Biophys. Acta* 1793, 27–32.
- Mishra, S., Murphy, L.C., Nyomba, B.L.G., Murphy, L.J., 2005. Prohibitin: a potential target for new therapeutics. *Trends Mol. Med.* 11, 192–197.
- Neboháčová, M., Maslov, D.A., Falick, A.M., Simpson, L., 2005. The effect of RNA interference down-regulation of RNA editing 3'-terminal uridylyl transferase (TUTase) 1 on mitochondrial *de novo* protein synthesis and stability of respiratory complexes in *Trypanosoma brucei*. *J. Biol. Chem.* 279, 7819–7825.
- Nijtmans, L.G.J., de Jong, L., Artal-Sanz, M., Coates, P.J., Berden, J.A., Back, J.W., Muijsers, A.O., van der Spek, H., Grivell, L.A., 2000. Prohibitins act as a membrane-bound chaperone for the stabilization of mitochondrial proteins. *EMBO J.* 19, 2444–2451.
- Osman, C., Wilmes, C., Tatsuta, T., Langer, T., 2007. Prohibitins interact genetically with Atp23, a novel processing peptidase and chaperone for the F<sub>1</sub>F<sub>0</sub>-ATP synthase. *Mol. Biol. Cell* 18, 627–633.
- Opperdoes, F.R., Michels, P.A., 2008. Complex I of Trypanosomatidae: does it exist? *Trends Parasitol.* 24, 310–317.
- Park, S.E., Xu, J., Frolova, A., Liao, L., O'Malley, B.W., Katzenellenbogen, B.S., 2005. Genetic deletion of the repressor of estrogen receptor activity (REA) enhances the response to estrogen in target tissues *in vivo*. *Mol. Cell Biol.* 25, 1989–1999.
- Ross, J.A., Nagy, Z.S., Kirken, R.A., 2008. The PHB1/2 phosphocomplex is required for mitochondrial homeostasis and survival of human T cells. *J. Biol. Chem.* 283, 4699–4713.
- Schleicher, M., Shepherd, B.R., Suarez, Y., Fernandez-Hernando, C., Yu, J., Pan, Y., Acevedo, L.M., Shadel, G.S., Sessa, W.C., 2008. Prohibitin-1 maintains the angiogenic capacity of endothelial cells by regulating mitochondrial function and senescence. *J. Cell Biol.* 180, 101–112.
- Schneider, A., Charriere, F., Pusnik, M., Horn, E.K., 2007. Isolation of mitochondria from procyclic *Trypanosoma brucei*. *Methods Mol. Biol.* 372, 67–80.
- Schumacher, M.A., Karamooz, E., Ziková, A., Trantírek, L., Lukeš, J., 2006. Crystal structures of *Trypanosoma brucei* MRP1/MRP2 guide-RNA-binding complex reveals RNA matchmaking mechanism. *Cell* 126, 701–711.
- Smalla, K.H., Mikhaylova, M., Sahin, J., Bernstein, H.G., Bogerts, B., Schmitt, A., van der Schors, R., Smit, A.B., Li, K.W., Gundelfinger, E.D., Kreutz, M.R., 2008. A comparison of the synaptic proteome in human chronic schizophrenia and rat ketamine psychosis suggest that prohibitin is involved in the synaptic pathology of schizophrenia. *Mol. Psychiatry* 13, 878–896.
- Smíd, O., Horáková, E., Vilímová, V., Hrdý, I., Cammack, R., Horváth, A., Lukeš, J., Tachezy, J., 2006. Knock-downs of mitochondrial iron-sulfur cluster assembly proteins IscS and IscU down-regulate the active mitochondrion of procyclic *Trypanosoma brucei*. *J. Biol. Chem.* 281, 28679–28686.
- Steglich, G., Neupert, W., Langer, T., 1999. Prohibitins regulate membrane protein degradation by the m-AAA protease in mitochondria. *Mol. Cell Biol.* 19, 3435–3442.
- Sun, Q.J., Miao, M.Y., Jia, X., Guo, W., Wang, L.H., Yao, Z.Z., Liu, C.L., Jiao, B.H., 2008. Subproteomic analysis of the mitochondrial proteins in rats 24 h after partial hepatectomy. *J. Cell. Biochem.* 105, 176–184.
- Tamura, K., Dudley, J., Nei, M., Kumar, S., 2007. MEGA4: molecular evolutionary genetics analysis (MEGA) software version 4.0. *Mol. Biol. Evol.* 24, 1596–1599.
- Tatsuta, T., Model, K., Langer, T., 2005. Formation of membrane-bound ring complexes by prohibitins in mitochondria. *Mol. Biol. Cell* 16, 248–259.
- Theiss, A.L., Idell, R.D., Srinivasan, S., Klapproth, J.M., Jones, D.P., Merlin, D., Sitarman, S.V., 2007. Prohibitin protects against oxidative stress in intestinal epithelial cells. *FASEB J.* 58, 197–206.
- Vondrušková, E., van den Burg, J., Ziková, A., Ernst, N.L., Stuart, K., Benne, R., Lukeš, J., 2005. RNA interference analyses suggest a transcript-specific regulatory role for mitochondrial RNA-binding proteins MRP1 and MRP2 in RNA editing and other RNA processing in *Trypanosoma brucei*. *J. Biol. Chem.* 280, 2429–2438.
- Ziková, A., Horáková, E., Jirků, M., Dunajčíková, P., Lukeš, J., 2006. The effect of down-regulation of mitochondrial RNA-binding proteins MRP1 and MRP2 on respiratory complexes in procyclic *Trypanosoma brucei*. *Mol. Biochem. Parasitol.* 149, 65–73.